electronics

Article

Adaptive NN Control of Electro-Hydraulic System with Full State Constraints

Chenyang Jiang, Shuai Sui and Shaocheng Tong *

School of Electrical Engineering, Liaoning University of Technology, Jinzhou 121001, China; jcy18524573892@163.com (C.J.); shuaisui2011@163.com (S.S.)
* Correspondence: jztongsc@163.com

Abstract: This paper presents an adaptive neural network (NN) control approach for an electro-hydraulic system. The friction and internal leakage are nonlinear uncertainties, and the states in the considered electro-hydraulic system are fully constrained. In the control design, the NNs are utilized to approximate the nonlinear uncertainties. Then, by constructing barrier Lyapunov functions and based on the adaptive backstepping control design technique, a novel adaptive NN control scheme is formulated. It has been proven that the developed adaptive NN control scheme can sustain the controlled electro-hydraulic system to be stable and make the system output track the desired reference signal. Furthermore, the system states do not surpass the given bounds. The computer simulation results verify the effectiveness of the proposed controller.

Keywords: adaptive neural network control; electro-hydraulic system; nonlinear uncertainties; state constraints

check for updates

Citation: Jiang, C.; Sui, S.; Tong, S. Adaptive NN Control of Electro-Hydraulic System with Full State Constraints. *Electronics* **2022**, *11*, 1483. https://doi.org/10.3390/electronics11091483

Academic Editor: Davide Astolfi

Received: 3 April 2022
Accepted: 1 May 2022
Published: 5 May 2022

1. Introduction

Electro-hydraulic systems are widely employed in sundry industrial applications such as robotic manipulators, active suspensions, precision machine tools, and aerospace systems. They provide many advantages over electric motors, including a high force to weight ratio, fast response time, and compact size. With the increasing applications of hydraulic mechanisms, the issue of stabilizing electro-hydraulic systems has attracted tremendous attention in recent years. To handle this issue, many control methods were developed. For instance, [1] presented a nonlinear adaptive robust control method for a single-rod electro-hydraulic actuator with unknown nonlinear parameters. By employing the control method and constructing a novel-type Lyapunov function, [2] developed an adaptive sliding mode control controller. In [3], an active fault-tolerant control (FTC) system is proposed against the valve faults of an independent metering valve. Backstepping control [4] was also widely used in EHS in handling mismatched disturbances. In [5], an output feedback nonlinear control is proposed for EHS, in which an extended state observer (ESO) and a nonlinear robust controller are synthesized via backstepping. In order to solve the uncertain nonlinearity and parameter uncertainty in hydraulic systems simultaneously, a nonlinear adaptive robust control method is presented in [6]. Further, a robust integral of the sign of the error controller and an adaptive controller is synthesized via the backstepping method for motion control of a hydraulic rotary actuator in [7], which theoretically guaranteed asymptotic tracking performance in the presence of various uncertainties. In [8], a practical nonlinear adaptive repetitive controller is proposed for motion control of hydraulic servo-mechanisms to learn and compensate for the periodic modeling uncertainties.

It should be mentioned that since the tolerance of the hydraulic rotary actuator is finite, the load pressure should be limited to a feasible boundary, and the rate limit of the hydraulic rotary actuator's response cannot be that large. To ensure that all the state variables are not violating their constraints and the normal operation of the controlled system, it is important to investigate the issue of state constraints in the control problem of EHS. In [9], a high-gain disturbance observer (HGDOB)-based backstepping controller was proposed for electro-hydraulic systems with position tracking error constraints. To suppress the violation of tracking error constraints, a barrier Lyapunov function-based dynamic surface control method was proposed for the position tracking control of the ammunition manipulator in [10].

Note that the control schemes mentioned above all require precise structural information of the considered hydraulic system. Especially, the frictions and internal leakage are both required to be known. Therefore, they do not effectively control the hydraulic systems with nonlinear uncertainties. Fuzzy systems [11] and neural networks [12–15] have good approximation performance, and thus they are frequently utilized to deal with uncertainties in nonlinear systems. In [16], the authors integrated fuzzy learning mechanisms into the modeling of EHS and proposed a kind of fuzzy PI controller. In [17], a neural adaptive control was developed for single-rod EHS to improve the dynamic tracking performance of the cylinder position under lumped uncertainties. Although these control methods improved the position tracking performance without precise knowledge of the EHS, they did not consider the control problem of EHS with state constraints.

Inspired by the above observations, this paper investigates the adaptive tracking control problem for an electro-hydraulic system with nonlinear uncertainties and full state constraints. By utilizing neural networks to model the nonlinear uncertainties, and constructing the barrier Lyapunov functions, an adaptive NN control approach is developed in the framework of adaptive backstepping control design. The main advantages of the proposed adaptive NN control scheme are as follows: it can ensure the controlled electro-hydraulic system is stable and make the system output track the desired reference signal. Furthermore, the system states are confined within the given compact sets and do not surpass their bounds. Note that the previous adaptive NN controller [17] also addressed the control problem for electro-hydraulic systems with lumped uncertainties by neural network approximation. However, detailed information such as the frictions and internal leakage was still required, the neural networks were merely utilized to approximate the lumped uncertainties composed of parameter uncertainties and the external disturbance. Furthermore, it did not consider the control problem for electro-hydraulic systems with state constraints. On the other hand, although [9] studied the control problem for electro-hydraulic systems with state constraints, it required the nonlinear dynamics of the electro-hydraulic system to be exactly known.

2. Problem Formulation and Preliminaries

2.1. Hydraulic System Model

The hydraulic system [5] under study is illustrated in Figure 1. On the left in Figure 1, an inertia load is driven by a servo valve-controlled hydraulic rotary actuator, whose schematic structure is presented on the right in Figure 1. The motion dynamics of the inertia load can be described by

$$J\ddot{y} = P_L D_m - F(y, \dot{y}) + f(t) \tag{1}$$

where J and y represent the moment of inertia and the angular displacement of the load, respectively; $P_L = P_1 - P_2$ is the load pressure of the hydraulic actuator, P_1 and P_2 are the pressures inside the two chambers of the actuator; D_m is the radian displacement of the actuator; F represents any continuous differentiable friction model, and f represents other disturbances. The load pressure dynamics can be written as

$$\frac{V_t}{4\beta_e}\dot{P}_L = -D_m\dot{y} - Q_t(P_L) + Q(t) + Q_L \tag{2}$$

where V_t is the total control volume of the actuator; β_e is the effective oil bulk modulus; $Q_t(P_L)$ is the total internal leakage of the actuator due to pressure; $Q(t)$ is the time-varying disturbances and external leakage; $Q_L = (Q_1 + Q_2)/2$ is the load flow, Q_1 is the supplied flow rate to the forward chamber, and Q_2 is the return flow rate of the return chamber. Q_L is related to the spool valve displacement of the servo valve, i.e., x_V, by

$$Q_L = k_q x_v \sqrt{P_s - sign(x_v) P_L} \tag{3}$$

where $k_q = C_d \omega \sqrt{1/\rho}$ is the flow gain, and $sign(x_v)$ is given as

$$sign(x_v) = \begin{cases} 1, & if\ x_v \geq 0 \\ -1, & if\ x_v < 0 \end{cases} \tag{4}$$

where C_d is the discharge coefficient; ω is the spool valve area gradient; ρ is the density of oil; P_s is the supply pressure of the fluid with respect to the return pressure P_r.

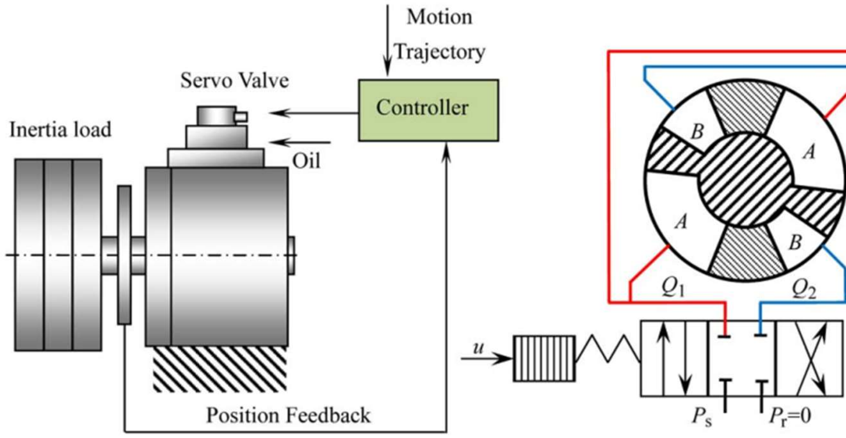

Figure 1. Architecture of the considered hydraulic system.

Although the model of servo valve dynamics is actually nonlinear, which has been considered by some researchers [6], only minimal performance improvement can be achieved for motion tracking, and additional sensors are required to obtain the spool position. Therefore, many studies neglect servo valve dynamics. So, in this paper, the relationship between the control applied to the servo valve and the spool position is defined as $x_v = k_i u$, i.e., the control applied to the servo valve is directly proportional to the spool position, where x_v is the spool position and u is the control input voltage, since a high-response servo valve is used here. Thus, (3) can be transformed to

$$Q_L = k_t u \sqrt{P_s - sign(u) P_L} \tag{5}$$

Since only variables y, $\dot{y}$ and P_L are necessary to be controlled for hydraulic motion systems, so defining the state variables as $X = [x_1, x_2, x_3]^T = [y, \dot{y}, D_m P_L / J]^T$ is sufficient for controller design. Then, the considered electro-hydraulic system can be expressed in a state-space form as

$$\begin{cases} \dot{x}_1 = x_2 \\ \dot{x}_2 = x_3 + \phi_1(x_2) + d_1(t) \\ \dot{x}_3 = g(x_3, u)u + \phi_2(x_2, x_3) + d_2(t) \end{cases} \tag{6}$$

where, $\phi_1(x_2) = -F(x_2)/J, d_1(t) = f(t)/J$, and

$$\phi_2(x_2, x_3) = -\frac{4D_m^2 \beta_e}{J V_t} x_2 - \frac{4\beta_e}{V_t} Q_t(x_3) \tag{7}$$

$$d_2(t) = 4\beta_e D_m Q(t)/(V_t J) \tag{8}$$

$$g(x_3,u)=\frac{4D_m\beta_e k_t}{JV_t}\sqrt{P_S-sign(u)Jx_3/D_m} \tag{9}$$

Remark 1. *It should be pointed out that the nonlinear friction models and the nonlinear internal leakage models used in this study are not considered by the previous studies. The nonlinear friction $F(x_2)$ and the nonlinear internal leakage $Q_t(x_3)$ are both considered nonlinear uncertainties. Thus, $\phi_1(x_2)$ and $\phi_2(x_2,x_3)$ in (6) are all unknown nonlinear functions.*

Assumption 1 [18]**.** *There exist positive constants A_0, A_1 and A_2 such that the given reference y_d and its derivatives satisfy $|y_d|\le A_0<k_{c1}$ and $\left|y_d^{(i)}\right|\le A_i(i=1,2)$.*

Assumption 2. *There exist positive constants k_{ci} such that the system states satisfy the restrictions: $|x_i|<k_{ci}$, $i=1,2,3$.*

Control Objective. The objective of this study is to propose an adaptive NN control scheme. The proposed adaptive NN control scheme can make the controlled electro-hydraulic system stable and y track the desired trajectory y_d. Moreover, the system states do not violate their bounds.

2.2. Radial Basis Function Neural Networks

A radial basis function neural network (RBFNN) [19] can be expressed as

$$\hat{f}(X|W)=W^TS(X) \tag{10}$$

where $X\in R^m$ is the input vector, $W\in R^r$ is the weight vector with neurons number r. $S(X)=[s_1(X),\ldots,s_r(X)]^T$, where $s_i(X)$ is a Gaussian-type basis function, which can be selected as

$$s_i(X)=\exp\left\{-\frac{(X-o_i)^T(X-o_i)}{\rho_i^2}\right\} \tag{11}$$

where ρ_i and $o_i\in R^m$ are the width of the Gaussian function and the center vector, respectively.

It is well known that an RBFNN can be used to approximate any a continuous function $F(X)$ as [20]

$$F(X)=W^{*T}S(X)+\varepsilon(X) \tag{12}$$

where W^* is the ideal constant vector and $\varepsilon(X)$ is the approximation error.

3. The Controller Design and Stability Analysis

3.1. Controller Design

Make the following variable transformation:

$$\begin{cases} z_1=x_1-y_d\\ z_2=x_2-\alpha_1\\ z_3=x_3-\alpha_2 \end{cases} \tag{13}$$

where y_d represents the desired trajectory, α_1 and α_2 represent the virtual control variables to be designed later.

Based on the above variable transformation, we will give the detailed three-step backstepping control [21] design procedures for the electro-hydraulic system (6).

Step 1: Noting (6), the time derivative of tracking error z_1 is

$$\dot{z}_1=x_2-\dot{y}_d \tag{14}$$

Construct a barrier Lyapunov function candidate as

$$V_1 = \frac{1}{2}\ln\frac{k_{b1}^2}{k_{b1}^2 - {z_1}^2} \tag{15}$$

where k_{b1} is a positive constant. It is obvious that in $\Omega_{z_1} : = \{z_1 : |z_1| < k_{b1}\}$, V_1 is a continuous differentiable. Then, the time derivative of V_1 can be derived as follows

$$\begin{aligned} \dot{V}_1 &= \tfrac{z_1\dot{z}_1}{k_{b1}^2 - z_1^2} \\ &= \tfrac{z_1}{k_{b1}^2 - z_1^2}(x_2 - \dot{y}_d) \\ &= \tfrac{z_1}{k_{b1}^2 - z_1^2}(z_2 + \alpha_1 - \dot{y}_d) \end{aligned} \tag{16}$$

Design the virtual controller α_1 as

$$\alpha_1 = \dot{y}_d - c_1 z_1 \tag{17}$$

where c_1 is a positive design parameter.

Step 2: From (6), the derivative of $z_2 = x_2 - \alpha_1$ with respect to time is given by

$$\begin{aligned} \dot{z}_2 &= x_3 + \phi_1(x_2) + d_1(t) - \dot{\alpha}_1 \\ &= z_3 + \alpha_2 + \phi_1(x_2) + d_1(t) - \dot{\alpha}_1 \end{aligned} \tag{18}$$

Based on the neural approximation, we can assume that

$$\phi_1(x_2) = {W_1^*}^T S_1(x_2) + \varepsilon_1(x_2) \tag{19}$$

where W_1^* denotes the ideal weight vector, $S_1(x_2) = [s_1(x_2), \ldots, s_{r_1}(x_2)]^T$ is the radial basis vector with Gaussian function $s_j(x_2)$, $j = 1, 2, \ldots, r_1$. ε_1 is the approximation error satisfying $|\varepsilon_1| \leq \bar{\varepsilon}_1$ with the constant $\bar{\varepsilon}_1 > 0$. Then (17) becomes

$$\dot{z}_2 = z_3 + \alpha_2 + {W_1^*}^T S_1(x_2) + \varepsilon_1(x_2) + d_1(t) - \dot{\alpha}_1 \tag{20}$$

Construct a barrier Lyapunov function candidate as

$$V_2 = \frac{1}{2}\ln\frac{k_{b2}^2}{k_{b2}^2(t) - {z_2}^2} + \frac{1}{2}\sigma_1 \widetilde{W}_1^T \widetilde{W}_1 \tag{21}$$

where σ_1 is a positive design parameter, and k_{b2} is a positive constant. In $\Omega_{z_2} : = \{z_2 : |z_2| < k_{b2}\}$, V_2 is a continuous differentiable. Then the time derivative of V_2 can be derived as

$$\dot{V}_2 = \frac{z_2\dot{z}_2}{k_{b2}^2 - z_2^2} + \sigma_1 \dot{\widetilde{W}}_1^T \widetilde{W}_1 \tag{22}$$

From (20) and (22), the following equation can be obtained

$$\dot{V}_2 = \frac{z_2}{k_{b2}^2 - z_2^2}(z_3 + \alpha_2 + {W_1^*}^T S_1(x_2) + \varepsilon_1(Z_1) + d_1(t) - \dot{\alpha}_1) + \sigma_1 \dot{\hat{W}}_1^T \widetilde{W}_1 \tag{23}$$

The virtual controller α_2 and the adaptive law of $\hat{W}_1$ are designed as

$$\alpha_2 = -c_2 z_2 - \hat{W}_1^T S_1(x_2) - \frac{z_2}{k_{b2}^2 - z_2^2} - \frac{k_{b2}^2 - z_2^2}{k_{b1}^2 - z_1^2} z_1 + \dot{\alpha}_1 \tag{24}$$

$$\dot{\hat{W}}_1 = \frac{1}{\sigma_1}\left(\frac{z_2}{k_{b2}^2 - z_2^2} S_1(x_2) - \tau_1 \hat{W}_1\right) \tag{25}$$

where c_2 and τ_1 are positive design parameters. $\hat{W}_1$ is the estimation of W_1^* and defined $\widetilde{W}_1 = \hat{W}_1 - W_1^*$.

Step 3: Noting (6), the time derivative of error $z_3 = x_3 - \alpha_2$ is

$$\dot{z}_3 = g(x_3, u)u + \phi_2(x_2, x_3) + d_2(t) - \dot{\alpha}_2 \tag{26}$$

Based on the virtual controller design in step 2, $\dot{\alpha}_2$ is given by

$$\dot{\alpha}_2 = \frac{\partial \alpha_2}{\partial x_1} x_2 + \frac{\partial \alpha_2}{\partial x_2} x_3 + \frac{\partial \alpha_2}{\partial \hat{W}_1} \dot{\hat{W}}_1 + \frac{\partial \alpha_2}{\partial y_d} \dot{y}_d + \frac{\partial \alpha_2}{\partial \dot{y}_d} \ddot{y}_d + h \tag{27}$$

where

$$h = \frac{\partial \alpha_2}{\partial x_2} \phi_1(x_2) + \frac{\partial \alpha_2}{\partial x_2} d_1(t) \tag{28}$$

Based on the neural approximation, it can be assumed that

$$\phi_2(Z_2) = W_2^{*T} S_2(Z_2) + \varepsilon_2(Z_2) \tag{29}$$

where $Z_2 = [x_2, x_3]^T$, and W_2^* denotes the ideal weight vector. $S_2(Z_2) = [s_1(Z_2), \ldots, s_{r_2}(Z_2)]^T$ is the radial basis vector with Gaussian function $s_j(Z_2),\ j = 1, 2, \ldots, r_2$. ε_2 is the approximation error satisfying $|\varepsilon_2| \le \bar{\varepsilon}_2$ with the constant $\bar{\varepsilon}_2 > 0$. Then (26) becomes

$$\dot{z}_3 = g(x_3, u)u + W_2^{*T} S_2(Z_2) + \varepsilon_2(Z_2) + d_2(t) - \dot{\alpha}_2 \tag{30}$$

Construct the barrier Lyapunov function candidate as

$$V_3 = \frac{1}{2} \ln \frac{k_{b3}^2}{k_{b3}^2(t) - {z_3}^2} + \frac{1}{2} \sigma_2 \widetilde{W}_2^T \widetilde{W}_2 \tag{31}$$

Similar to Step 2, the time derivative of V_3 is

$$\dot{V}_3 = \frac{z_3 \dot{z}_3}{k_{b3}^2 - z_3^2} + \sigma_2 \dot{\widetilde{W}}_2^T \widetilde{\xi}_2 \tag{32}$$

where σ_2 is a positive design parameter, and k_{b3} is a positive constant. In $\Omega_{z_3} := \{z_3 : |z_3| < k_{b3}\}$, V_3 is a continuous differentiable. Substituting (30) into (32) leads to

$$\dot{V}_3 = \frac{z_3}{k_{b3}^2 - z_3^2} (g(x_3, u)u + W_2^{*T} S_2(Z_2) + \varepsilon_2(Z_2) + d_2(t) - \dot{\alpha}_2) + \sigma_2 \dot{\hat{W}}_2^T \widetilde{W}_2 \tag{33}$$

The actual controller V_3 and the adaptive law are designed as follows.

$$u = -\frac{1}{g(x_3, u)} \left[c_3 z_3 + \hat{W}_2^T S_2(Z_2) + \frac{z_3}{k_{b3}^2 - z_3^2} + \frac{(k_{b3}^2 - z_3^2)}{(k_{b2}^2 - z_2^2)} z_2 + \Xi \right] \tag{34}$$

where

$$\begin{aligned} \Xi = {} & \tfrac{\partial \alpha_2}{\partial x_1} x_2 + \tfrac{\partial \alpha_2}{\partial x_2} x_3 + \tfrac{\partial \alpha_2}{\partial \hat{W}_1} \dot{\hat{W}}_1 + \tfrac{\partial \alpha_2}{\partial y_d} \dot{y}_d + \tfrac{\partial \alpha_2}{\partial \dot{y}_d} \ddot{y}_d \\ & - \tfrac{z_3}{k_{b3}^2 - z_3^2} \left(\tfrac{\partial \alpha_2}{\partial x_2} \right)^2 - \tfrac{z_3}{2(k_{b3}^2 - z_3^2)} \left(\tfrac{\partial \alpha_2}{\partial x_2} \right)^2 \| S_1(x_2) \|^2 \end{aligned}$$

$$\dot{\hat{W}}_2 = \frac{1}{\sigma_2} \left(\frac{z_3}{k_{b3}^2 - z_3^2} S_2(Z_2) - \tau_2 \hat{W}_2 \right) \tag{35}$$

where c_3 and τ_2 are positive design parameters. $\hat{W}_3$ is the estimation of W_3^* and defined $\widetilde{W}_3 = \hat{W}_3 - W_3^*$. In practice, P_1 and P_2 are both bounded by P_s and $|P_L|$ is sufficiently smaller than P_s to ensure that the positive function $g(x_3, u)$ is far away from zero [5].

The developed adaptive NN backstepping control scheme via the above three-step backstepping control design procedures are shown in Figure 2.

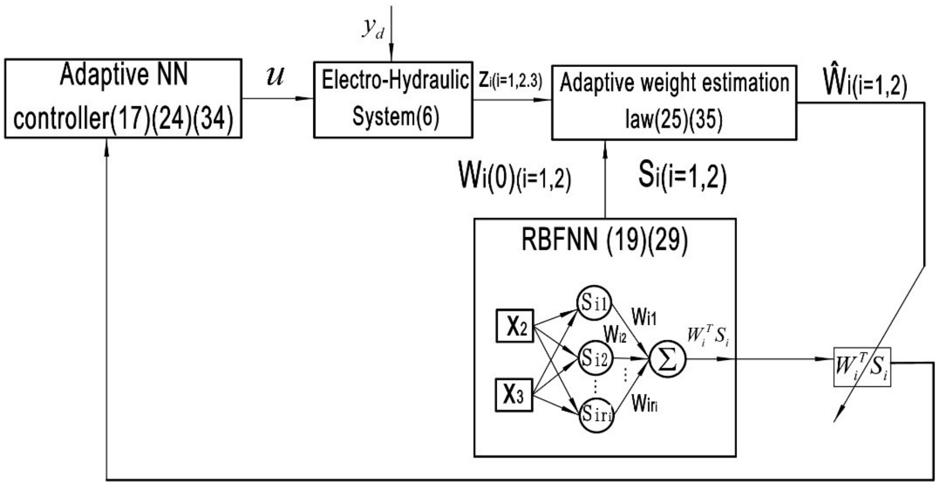

Figure 2. The block diagram of the neural adaptive network control scheme.

3.2. Stability Analysis

The properties of the proposed adaptive NN backstepping control method are given by the following Theorem.

Theorem 1. *Consider electro-hydraulic system (6) under Assumptions 1–2, if we adopt the virtual controllers (17), (24), the actual controller (34), and parameter adaptive laws (25), (35), then the following properties can be guaranteed:*

1. *All the variables in the closed-loop system are bounded and are always confined in their respective compact sets;*
2. *The tracking error converges to a neighborhood of zero, which can be made arbitrarily small by appropriately selecting design parameters.*

Proof of Theorem 1. Considering Lyapunov function as $V = \sum_{i=1}^{3} V_i$. With (16), (23), and (33) we have

$$\begin{aligned}\dot{V} = & \tfrac{z_3}{k_{b3}^2 - z_3^2}\left(g(x_3,u)u + W_2^{*T} S_2(Z_2) + \varepsilon_2(Z_2) + d_2(t) - \dot{\alpha}_2\right) \\ & + \tfrac{z_2}{k_{b2}^2 - z_2^2}\left(z_3 + \alpha_2 + W_1^{*T} S_1(Z_1) + \varepsilon_1(Z_1) + d_1(t) - \dot{\alpha}_1\right) \\ & + \tfrac{z_1}{k_{b1}^2 - z_1^2}\left(z_2 + \alpha_1 - \dot{y}_d\right) + \sigma_1 \dot{\hat{W}}_1^T \widetilde{W}_1 + \sigma_2 \dot{\hat{W}}_2^T \widetilde{W}_2\end{aligned} \quad (36)$$

Substituting (17), (24), (25), (34), and (35) into (36), the following inequality can be derived

$$\begin{aligned}\dot{V} \leq & -\sum_{i=1}^{3} \tfrac{c_i z_i^2}{k_{bi}^2 - z_i^2} - \sum_{i=1}^{2} \tau_i \hat{W}_i^T \widetilde{W}_i \\ & + \overline{\varepsilon}_1^2 + \overline{d}_1^2 + \tfrac{1}{2}\overline{\varepsilon}_2^2 + \tfrac{1}{2}\overline{d}_2^2 + \tfrac{1}{2}\left\|W_1^*\right\|^2\end{aligned} \quad (37)$$

By applying Young's inequality, it has

$$-\tau_i \widetilde{W}_i^T \hat{W}_i \leq \frac{-\tau_i \left\|\widetilde{W}_i\right\|^2}{2} + \frac{\tau_i \left\|W_i^*\right\|^2}{2} \quad (38)$$

Based on (38), (37) can be derived as

$$\begin{aligned} \dot{V} \quad & \leq -\sum_{i=1}^{3} \frac{c_i z_i^2}{k_{bi}^2 - z_i^2} - \frac{1}{2}\sum_{i=1}^{2} \tau_i \left\| \widetilde{W}_i \right\|^2 + \frac{1}{2}\sum_{i=1}^{2} \tau_i \left\| W_i^* \right\|^2 \\ & + \bar{\varepsilon}_1^2 + \bar{d}_1^2 + \frac{1}{2}\bar{\varepsilon}_2^2 + \frac{1}{2}\bar{d}_2^2 + \frac{1}{2}\left\| W_1^* \right\|^2 \end{aligned} \tag{39}$$

From (15), (21), and (31), we can obtain

$$V = \frac{1}{2}\sum_{i=1}^{3} \ln \frac{k_{bi}^2}{k_{bi}^2(t) - z_i{}^2} + \frac{1}{2}\sum_{i=1}^{2} \sigma_i \widetilde{W}_i^T \widetilde{W}_i \tag{40}$$

In [22], it has been proven that $\ln \frac{k_{bi}^2}{k_{bi}^2 - z_i^2} \leq \frac{z_i^2}{k_{bi}^2 - z_i^2}$. Thus, we have

$$V \leq \frac{1}{2}\sum_{i=1}^{3} \frac{z_i^2}{k_{bi}^2 - z_i^2} + \frac{1}{2}\sum_{i=1}^{2} \sigma_i \widetilde{W}_i^T \widetilde{W}_i \tag{41}$$

Define $a = \min\{2c_1, 2c_2, 2c_3, \tau_1/\sigma_1, \tau_2/\sigma_2\}$ and $b = \bar{\varepsilon}_1^2 + \bar{d}_1^2 + \frac{1}{2}\bar{\varepsilon}_2^2 + \frac{1}{2}\bar{d}_2^2 + \frac{1}{2}\left\| W_1^* \right\|^2 + \frac{1}{2}\sum_{i=1}^{2} \tau_i \left\| W_i^* \right\|^2$. Therefore, the following inequality holds

$$\dot{V} \leq -aV + b \tag{42}$$

From (42) and similar to [23,24] we obtain that all the signals of the closed-loop system are bounded.

Further, based on (42), it can be obtained

$$\ln \frac{k_{b1}^2}{k_{b1}^2 - z_1^2} \leq 2V(0)e^{-at} + 2b/a \tag{43}$$

That is,

$$\frac{k_{b1}^2}{k_{b1}^2 - z_1^2} \leq e^{2V(0)e^{-at} + 2b/a} \tag{44}$$

From (44), it yields

$$|z_1| \leq k_{b1}\sqrt{1 - e^{-2(V(0)e^{-at} + b/a)}} \tag{45}$$

As $t \to \infty$, we can obtain $|z_1| \leq k_{b1}\sqrt{1 - e^{-2b/a}}$, thus z_1 can be made arbitrarily small by selecting the design parameters appropriately.

Additionally, from $z_1 = x_1 - y_d$ and $|y_d| \leq A_0$ in Assumption 1, we can obtain $|x_1| < k_{b1} + A_0$. Define $k_{c1} = k_{b1} + A_0$, then $|x_1| < k_{c1}$. Moreover, from (17), (24), there must exist constants $B_{i-1} > 0$ such that $|\alpha_{i-1}| \leq B_{i-1}$, $i = 2, 3$. Then, according to $z_i = x_i - \alpha_{i-1}$, it can be derived that $|x_i| < B_{i-1} + k_{bi}$. Define $k_{c1} = k_{b1} + A_0$, then we can also obtain $|x_i| \leq k_{ci}$, $i = 2, 3$. Therefore, we can conclude that all the states do not violate their prescribed bounds. □

4. Simulation Studies

In order to verify the effectiveness of the proposed neural adaptive controller, computer simulations are carried out. In the simulations, parameters of the electro-hydraulic system to be controlled are chosen with reference to a previous study [5], which are listed in Table 1.

Table 1. Parameters of the Simulation System.

Physical Parameter	Value
$J(\mathrm{kg}\cdot\mathrm{m}^2)$	0.2
$D_m(\mathrm{m}^3/\mathrm{rad})$	5.8×10^{-5}
$C_t(\mathrm{m}^3/\mathrm{s}/\mathrm{Pa})$	1.0×10^{-12}
$k_t(\mathrm{m}^3/\mathrm{s}/\mathrm{V}/\mathrm{Pa}^{-1/2})$	1.1969×10^{-8}
$B(\mathrm{N}\cdot\mathrm{m}\cdot\mathrm{s}/\mathrm{rad})$	90
$\beta_e(\mathrm{Pa})$	7.0×10^{8}
$V_t(\mathrm{m}^3)$	1.16×10^{-4}
$P_s(\mathrm{Pa})$	1.0×10^{7}

The two layers' RBFNNs $\hat{f}_1(x_2\big|\hat{W}_1)=\hat{W}_1^T S_1(x_2)$ and $\hat{f}_2(Z_2\big|\hat{W}_1)=\hat{W}_2^T S_2(Z_2)$ contain five nodes with the centers spaced in the interval $[-2,2]$ and the widths of the Gaussian function are selected as 5. The radial basis functions are chosen as follows.

$$s_{1,j}(x_2)=\exp\left[-\frac{(x_2-o_{1,j})^2}{5}\right] \tag{46}$$

$$s_{2,j}(x_2,x_3)=\exp\left[-\frac{(x_2-o_{2,j})^2}{5}\right]\times\exp\left[-\frac{(x_3-o_{2,j})^2}{5}\right] \tag{47}$$

where $o_{1,j}=-3+j, j=1,\ldots,5$ are centers of the nodes in RBFNN $\hat{f}_1(x_2\big|\hat{W}_1)=\hat{W}_1^T S_1(x_2)$, $o_{2,j}=-3+j, j=1,\ldots,5$ are centers of the nodes in RBFNN $\hat{f}_2(Z_2\big|\hat{W}_1)=\hat{W}_2^T S_2(Z_2)$.

The virtual control laws and the actual controller are designed as follows

$$\alpha_1=\dot{y}_d-c_1z_1 \tag{48}$$

$$\alpha_2=-c_2z_2-\hat{W}_1{}^T S_1(Z_1)-\frac{z_2}{k_{b2}^2-z_2^2}-\frac{k_{b2}^2-z_2^2}{k_{b1}^2-z_1^2}z_1+\dot{\alpha}_1 \tag{49}$$

$$u=-\frac{1}{g(x_3,u)}\left[k_3z_3+\hat{W}_2{}^T S_2(Z_2)+\frac{z_3}{k_{b3}^2-z_3^2}+\frac{(k_{b3}^2-z_3^2)}{(k_{b2}^2-z_2^2)}z_2+\Xi\right] \tag{50}$$

where

$$\begin{aligned}\Xi=&\tfrac{\partial\alpha_2}{\partial x_1}x_2+\tfrac{\partial\alpha_2}{\partial x_2}x_3+\tfrac{\partial\alpha_2}{\partial\hat{W}_1}\dot{\hat{W}}_1+\tfrac{\partial\alpha_2}{\partial y_d}\dot{y}_d+\tfrac{\partial\alpha_2}{\partial\dot{y}_d}\ddot{y}_d\\&-\tfrac{z_3}{k_{b3}^2-z_3^2}\left(\tfrac{\partial\alpha_2}{\partial x_2}\right)^2-\tfrac{z_3}{2(k_{b3}^2-z_3^2)}\left(\tfrac{\partial\alpha_2}{\partial x_2}\right)^2\|S_1(x_2)\|^2\end{aligned}$$

The parameter adaptive laws are given as

$$\dot{\hat{W}}_1=\frac{1}{\sigma_1}\left(\frac{z_2}{k_{b2}^2-z_2^2}S_1(x_2)-\tau_1\hat{W}_1\right) \tag{51}$$

$$\dot{\hat{W}}_2=\frac{1}{\sigma_2}\left(\frac{z_3}{k_{b3}^2-z_3^2}S_2(Z_2)-\tau_2\hat{W}_2\right) \tag{52}$$

The design parameters in (48)–(52) are listed in Table 2.

The desired trajectory is selected as $y_d(t)=(8\sin(3.28t)+2\cos(6.28t))^\circ$, and the state constraints are given as $|x_1|\le k_{c1}=11^\circ$, $|x_2|\le k_{c2}=40^\circ/\mathrm{s}$ and $|x_3|\le k_{c3}=18000\ \mathrm{N}/(\mathrm{rad}\cdot\mathrm{kg}\cdot\mathrm{m})$.

Table 2. Design Parameters.

	Parameters	Values
Parameters of the virtual and actual controllers	c_1	226
	c_2	215
	c_3	256
Parameters of parameter adaptive laws	σ_1^{-1}	1.7
	σ_2^{-1}	1.5
	τ_1	2.6
	τ_2	2.3

In the simulation, the initial values of the state variables are given as $x_1(0) = 2°$, $x_2(0) = 10°/\mathrm{s}$, $x_3(0) = 10000\ \mathrm{N}/(\mathrm{rad}\cdot\mathrm{kg}\cdot\mathrm{m})$, while the initial values of the adaptive parameters W_1 and W_2 are selected as $W_1(0) = [1,2,3,8,2]^T$, $W_2(0) = [10,8,1,7,15]^T$.

The simulation results are shown in Figures 3–7. Figure 3 shows the trajectories of the output and tracking signals. It can be seen from Figure 3 that the proposed scheme has a good tracking performance. Figures 4 and 5 draw the trajectories of x_2 and x_3. Figures 3–5 illustrate that the given constraint bounds of the state variables are not violated. Figures 6 and 7 depict the trajectories of the actual controller $u(t)$, parameters $\hat{W}_1$ and $\hat{W}_2$, respectively.

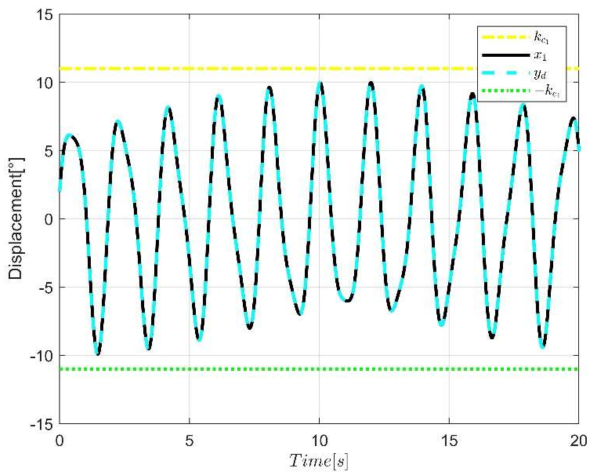

Figure 3. The trajectories of x_1 and y_d.

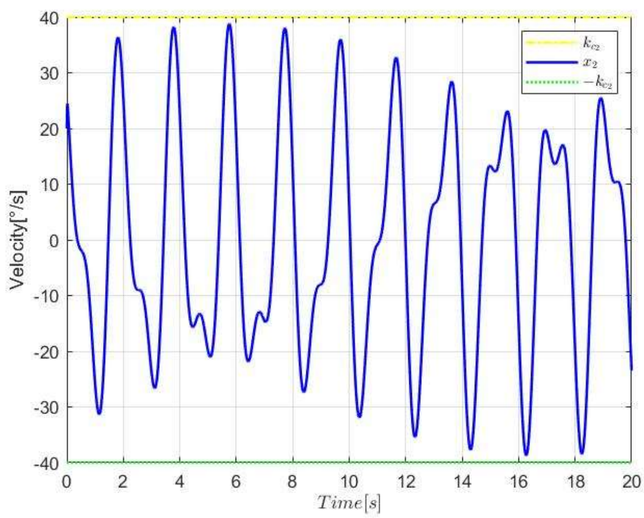

Figure 4. The trajectory of x_2.

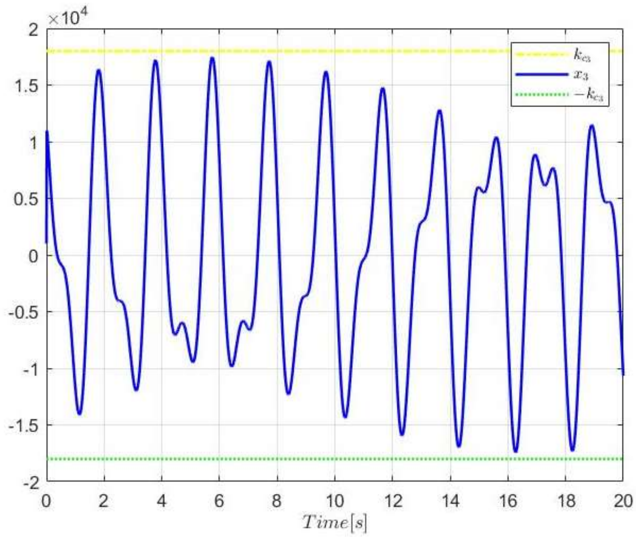

Figure 5. The trajectory of x_3.

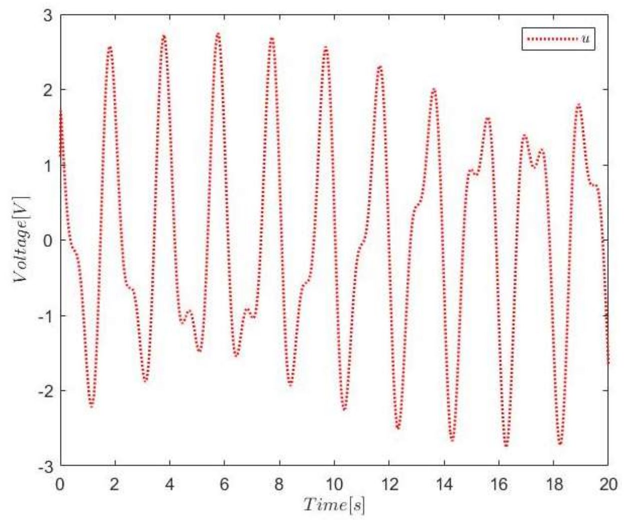

Figure 6. The trajectory of u.

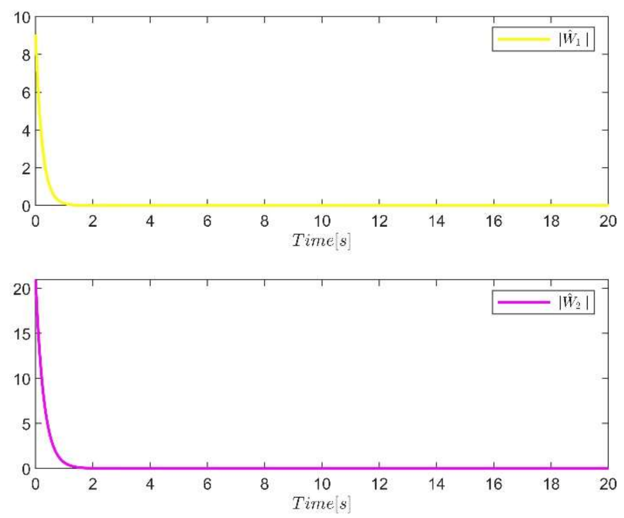

Figure 7. The trajectories of $\|\hat{W}_1\|$ and $\|\hat{W}_2\|$.

Furthermore, to illustrate the effectiveness of the proposed adaptive NN control scheme, we made a simulation comparison with an adaptive control scheme without the state constraints. In the simulation, all the design parameters and initial conditions of the states and parameters are chosen the same as in the above simulation. The simulation results are shown in Figures 8–11.

Comparing Figures 3 and 8, it is easy to find that the two control schemes can both guarantee good tracking performance, but the proposed scheme has a more satisfactory performance. By analyzing Figures 3–5 and 8–10 we can find that the proposed control scheme can sustain the states x_i, $i = 1, 2, 3$ not to surpass their bounds k_{ci}. While the states of the adaptive NN scheme without state constraint violate their bounds in transient conditions. In fact, the state variables surge in the beginning and slightly surpass the constraints, which means that the angular velocity and the load pressure surge too high in the transient conditions, which will do harm to the normal operation of EHS. In addition, from Figures 6 and 11, we can see that the control signal of the proposed adaptive NN control scheme is kept in a reasonable scope of [−3, 3]. However, the input voltage in the adaptive NN control scheme without state constraints spreads in the interval of [14,21], which indicates that the adaptive NN control scheme with state constraints requires less control energy to stabilize the electro-hydraulic system than the one without state constraints.

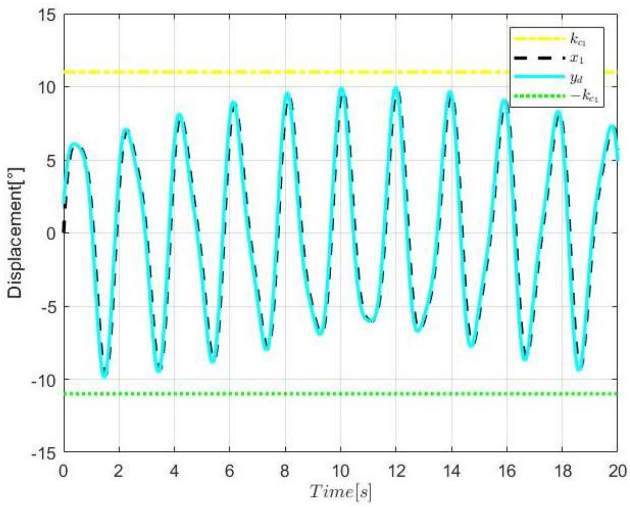

Figure 8. The trajectory of x_1 in control scheme without state constraints.

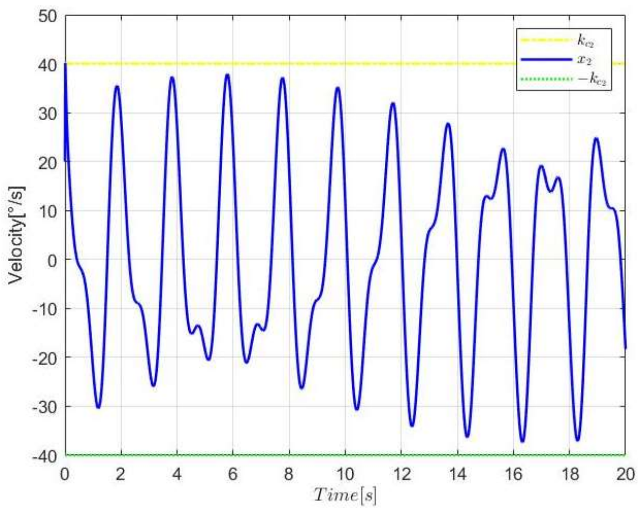

Figure 9. The trajectory of x_2 in control scheme without state constraints.

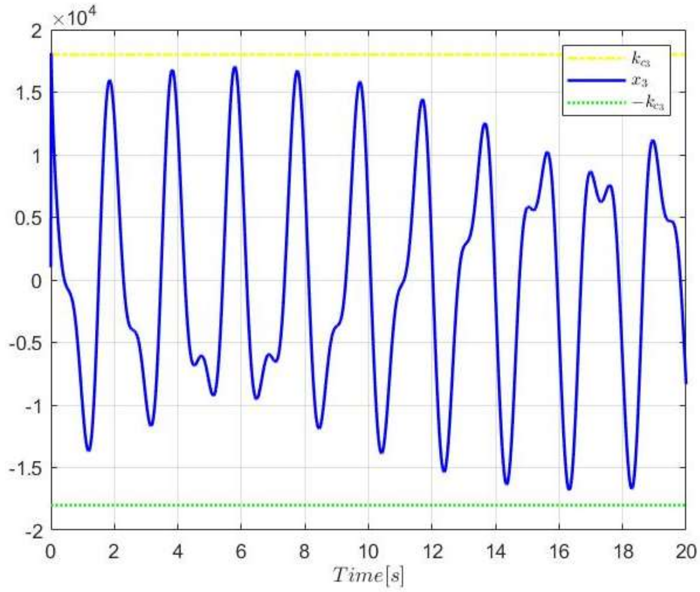

Figure 10. The trajectory of x_3 in control scheme without state constraints.

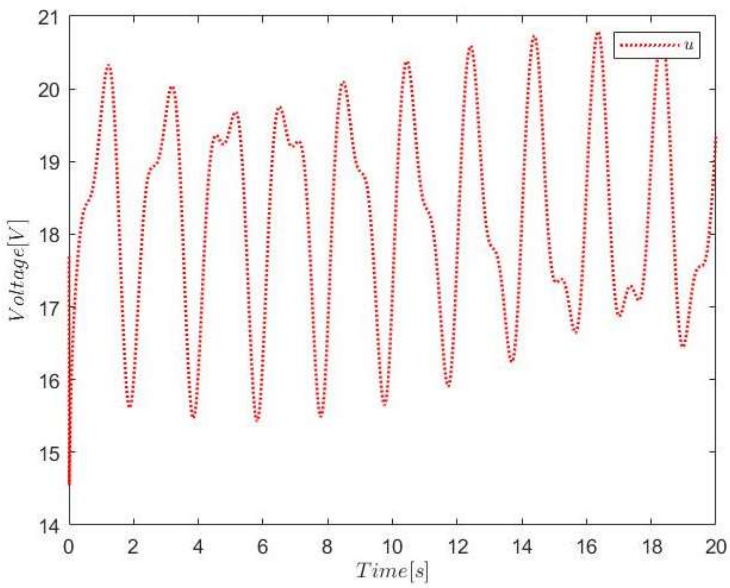

Figure 11. The trajectory of u in control scheme without state constraints.

5. Conclusions

This paper investigated an adaptive NN backstepping control problem for an electro-hydraulic system driven by a dual-vane hydraulic rotary actuator, in which the states are fully constrained, and the friction and internal leakage are nonlinear uncertainties. The neural networks are exploited to approximate the unknown nonlinear uncertainties, and by constructing suitable barrier Lyapunov functions, a novel adaptive NN backstepping control scheme has been developed, which can guarantee the controlled electro-hydraulic system to be stable and the tracking error to converge to a smaller neighborhood of zero. Meanwhile, the state variables are constrained in bounded compact sets. Comparative simulation results have checked the effectiveness of the proposed control method. Our further research work will focus on the finite-time intelligent output control design for electro-hydraulic systems with unmeasurable states.

Author Contributions: Conceptualization, C.J.; formal analysis, S.T.; writing-original draft preparation, S.S. and S.T.; review and editing, C.J., S.S. and S.S. All authors have read and agreed to the published version of the manuscript.

Funding: This work was funded in part by the National Natural Science Foundation of China (Nos. 62173172 and 62176111), in part by the Doctoral Research Initiation of Foundation of Liaoning Province, China, under Grant 2021-BS-260, in part by the general project of Liaoning Provincial Department of Education, under Grant LJKZ0627.

Acknowledgments: The authors thank the anonymous reviewers for their useful comments that improved the quality of the paper.

Conflicts of Interest: The authors declare no conflict of interest.

References

1. Guan, C.; Pan, S. Nonlinear adaptive robust control of single-rod electro-hydraulic actuator with unknown nonlinear parameters. *IEEE Trans. Control Syst. Technol.* **2008**, *16*, 434–445. [CrossRef]
2. Guan, C.; Pan, S. Adaptive sliding mode control of electro-hydraulic system with nonlinear unknown parameters. *Control Eng. Pract.* **2008**, *16*, 1275–1284. [CrossRef]
3. Ding, R.; Cheng, M.; Jiang, L.; Hu, G. Active fault-tolerant control for electro-hydraulic systems with an independent metering valve against valve faults. *IEEE Trans. Ind. Electron.* **2021**, *68*, 7221–7232. [CrossRef]
4. Guo, Q.; Zhang, Y.; Celler, B.G.; Su, S.W. Backstepping control of electro-hydraulic system based on extended-state-observer with plant dynamics largely unknown. *IEEE Trans. Ind. Electron.* **2016**, *63*, 6909–6920. [CrossRef]
5. Yao, J.; Jiao, Z.; Ma, D. Extended-state-observer-based output feedback nonlinear robust control of hydraulic systems with backstepping. *IEEE Trans. Ind. Electron.* **2014**, *61*, 6285–6293. [CrossRef]
6. Yao, B.; Bu, F.; Reedy, J.; Chiu, G.T.C. Adaptive robust motion control of single-rod hydraulic actuators: Theory and experiments. *IEEE/ASME Trans. Mechatron.* **2000**, *5*, 79–91.
7. Yao, J.; Jiao, Z.; Ma, D.; Yan, L. High-accuracy tracking control of hydraulic rotary actuators with modelling uncertainties. *IEEE/ASME Trans. Mechatron.* **2014**, *19*, 633–641. [CrossRef]
8. Yao, J.; Jiao, Z.; Ma, D. A practical nonlinear adaptive control of hydraulic servomechanisms with periodic-like disturbances. *IEEE/ASME Trans. Mechatron.* **2015**, *20*, 2752–2760. [CrossRef]
9. Won, D.; Kim, W.; Shin, D.; Chung, C.C. High-gain disturbance observer-based backstepping control with output tracking error constraint for electro-hydraulic systems. *IEEE Trans. Control Syst. Technol.* **2015**, *23*, 787–795. [CrossRef]
10. Nie, S.; Qian, L.; Chen, L.; Tian, L.; Zou, Q. Barrier Lyapunov functions-based dynamic surface control with tracking error constraints for ammunition manipulator electro-hydraulic system. *Def. Technol.* **2021**, *17*, 836–845. [CrossRef]
11. Song, Y.; Hu, Z.; Ai, C. Fuzzy Compensation and Load Disturbance Adaptive Control Strategy for Electro-Hydraulic Servo Pump Control System. *Electronics* **2022**, *11*, 1159. [CrossRef]
12. Botmart, T.; Sabir, Z.; Raja, M.A.Z.; Weera, W.; Sadat, R.; Ali, M.R. A Numerical Study of the Fractional Order Dynamical Nonlinear Susceptible Infected and Quarantine Differential Model Using the Stochastic Numerical Approach. *Fractal Fract.* **2022**, *6*, 139. [CrossRef]
13. Sabir, Z.; Botmart, T.; Raja, M.A.Z.; Weera, W.; Sadat, R.; Ali, M.R.; Alsulami, A.A.; Alghamdi, A. Artificial neural network scheme to solve the nonlinear influenza disease model. *Biomed. Signal Processing Control* **2022**, *75*, 103594. [CrossRef]
14. Sabir, Z.; Baleanu, D.; Ali, M.R.; Sadat, R. A novel computing stochastic algorithm to solve the nonlinear singular periodic boundary value problems. *Int. J. Comput. Math.* 2022. [CrossRef]
15. Zhang, Z.; Peng, L.; Zhang, J.; Wang, X. Finite-Time Neural Network Fault-Tolerant Control for Robotic Manipulators under Multiple Constraints. *Electronics* **2022**, *11*, 1343. [CrossRef]
16. Costa Branco, P.J.; Dente, J.A. On using fuzzy logic to integrate learning mechanisms in an electro-hydraulic system. I. actuator's fuzzy modeling. *IEEE Trans. Syst. Man Cybern. Part C (Appl. Rev.)* **2000**, *30*, 305–316.
17. Guo, Q.; Chen, Z. Neural adaptive control of single-rod electrohydraulic system with lumped uncertainty. *Mech. Syst. Signal Processing* **2021**, *146*, 106869. [CrossRef]
18. Min, H.; Xu, S.; Zhang, Z. Adaptive finite-time stabilization of stochastic nonlinear systems subject to full-state constraints and input saturation. *IEEE Trans. Autom. Control* **2021**, *66*, 1306–1313. [CrossRef]
19. Chen, S.; Wu, Y.; Luk, B.L. Combined genetic algorithm optimization and regularized orthogonal least squares learning for radial basis function networks. *IEEE Trans. Neural Netw.* **1999**, *10*, 1239–1243. [CrossRef]
20. Li, Y.; Wang, T.; Liu, W.; Tong, S. Neural network adaptive output-feedback optimal control for active suspension systems. *IEEE Trans. Syst. Man Cybern. Syst.* **2021**, 1–12. [CrossRef]
21. Li, Y.; Liu, Y.; Tong, S. Observer-based neuro-adaptive optimized control of strict-feedback nonlinear systems with state constraints. *IEEE Transactions on Neural Networks and Learning Systems* **2021**, 1–15. [CrossRef] [PubMed]
22. Ren, B.; Ge, S.S.; Tee, K.P.; Lee, T.H. Adaptive neural control for output feedback nonlinear systems using a barrier Lyapunov function. *IEEE Trans. Neural Netw.* **2010**, *21*, 1339–1345. [PubMed]

23. Liu, Y.-J.; Li, J.; Tong, S.; Chen, C.L.P. Neural network control-based adaptive learning design for nonlinear systems with full-state constraints. *IEEE Trans. Neural Netw. Learn. Syst.* **2016**, *27*, 1562–1571. [CrossRef] [PubMed]
24. Liu, Y.-J.; Zhao, W.; Liu, L.; Li, D.; Tong, S.; Chen, C.L.P. Adaptive Neural Network Control for a Class of Nonlinear Systems with Function Constraints on States. *IEEE Trans. Neural Netw. Learn. Syst.* **2021**, 1–10. [CrossRef] [PubMed]